CrystEngComm

Accepted Manuscript

This article can be cited before page numbers have been issued, to do this please use: S. Coles, P. A. Gale, I. Kirby, M. Pitak and C. Wilson, *CrystEngComm*, 2015, DOI: 10.1039/C5CE00213C.

ROYAL SOCIETY OF CHEMISTRY

www.rsc.org/crystengcomm

Journal Name CrystEngComm
Dynamic Article Links ►
View Article Online
DOI: 10.1039/C5CE00213C

Cite this: DOI: 10.1039/c0xx00000x

www.rsc.org/xxxxxx

ARTICLE TYPE

Electron density distribution studies as a tool to explore the behaviour of thiourea-based anion receptors

Isabelle L. Kirby,[a] Mateusz B. Pitak,[a] Claire Wilson[b], Philip A. Gale[a] and Simon J. Coles*[a]

Received (in XXX, XXX) Xth XXXXXXXXX 20XX, Accepted Xth XXXXXXXXX 20XX
DOI: 10.1039/b000000x

Building on previous studies of anion-receptor complexes based on a urea scaffold substituted symmetrically with electron-withdrawing nitro groups, the electron density distribution in an analogous thiourea receptor complex and the related asymmetrically substituted urea and thiourea receptors are described. On this basis it is possible to probe both the effect of changing the receptor core from a urea to a thiourea moiety and that of asymmetrical substitution of the receptor molecule. These modifications are shown to significantly alter the anion binding properties, solid-state packing and electron density distribution in the anion-receptor complexes.

Introduction

Anion receptor chemistry has a broad range of applications including catalysis, sensing and transport.[1] Ureas and thioureas are frequently used because of their strong hydrogen bond donor ability and easy synthetic modification.[2] While the structural properties of ureas in the solid-state have been widely studied, including their co-crystal structures with hydrogen bond acceptor molecules[3, 4], the properties of analogous thioureas have been much less explored[5, 6]. There are a number of differences between ureas and thioureas that could be expected to alter the solid-state structures of their analogous compounds. Thiourea N−H bonds are more acidic than those in ureas and hence thioureas are stronger hydrogen bond donors. However sulfur is a less effective hydrogen bond acceptor than oxygen. In the crystal structures of urea containing compounds the most prominent motif is that of the linear planar α-tape, while in analogous thioureas zig-zag chains or dimer motifs are commonly observed. This is due to the *trans-trans* conformation adopted by N,N'-disubstituted ureas whereas the analogous thioureas exist in solution as a mixture of three rotamers, the *trans-trans*, the *trans-cis* and the *cis-cis*. Custelcean *et al.*, have shown that by varying the steric bulk of the substituent in N, N'-disubstituted thioureas one can control the hydrogen bonding motif present in the crystal structure.[6]

Recently we have studied the anion binding ability of a series of N,N'-diphenyl substituted symmetrical urea receptors in both solution and the solid-state.[7, 8] This systematic study investigates the effect of altering the substituent position on the electron density distribution across the anion-receptor complexes, the crystal packing arrangements and anion binding ability of the receptors and attempts to correlate these properties. The strength of the anion binding in the solid-state was derived using the methods associated with the Quantum Theory of Atoms of Molecules (QTAIM). Increasing the basicity, by altering the anion, was shown for the first time in the solid-state to cause an increase in hydrogen bond strength using this method.[8] The family of anion-receptors studied has been extended to include thiourea molecules and comparisons made between the electron density distribution in anion-receptor complexes of urea and analogous thiourea receptors. In the previous study, the phenyl rings of the urea receptor molecules were symmetrically functionalised with nitro functional groups. These electron-withdrawing groups were included to increase the acidity of the N−H bonds, which act as hydrogen bond donors and associate with anions. The effect of altering the position of the electron-withdrawing group was investigated. However, there is also interest in investigating the effect that asymmetric substitution of the phenyl rings has on both the anion binding strength of the receptors and on the charge density distribution across the receptor molecule. These relatively simple anion-receptors are used as models to understand the more complex systems found in anion-receptor chemistry and to explain the effect of structural modifications.

For this reason, receptor **1** (1-(4-nitrophenyl)-3-phenylurea) and **2** (1-(4-nitrophenyl)-3-phenylthiourea) shown in Figure 1 were synthesised. The crystal structures of the chloride complexes of both receptors were obtained, in addition to those of the receptor molecules, and the electron density distribution in these complexes modelled using the Hansen-Coppens[9] formalism (**4**) and Invariom[10] method (**3**). The chloride complex of the symmetrical receptor,1,3-bis(4-nitrophenyl)thiourea **8**, is also included and comparison made with previously described[8] urea-based chloride complex **7**.

Here, a comparison between the crystal packing arrangements in the receptor only and the complexed structures is discussed, along with the anion binding abilities of the receptors. The electron density distributions in the urea structures (**3** and **7**) are compared to the thiourea structures (**4** and **8**) and symmetrical substitution contrasted to asymmetric substitution (**7** and **8** *vs.* **3** and **4**).

The choice of counterion in these four anion-receptor complexes

View Article Online
DOI: 10.1039/C5CE00213C

is either the tetramethylammonium (TMA) cation found in **4** and **7** or the tetraethylammonium cation (TEA) present in **3** and **8** and is based on solubility and crystallisation considerations.

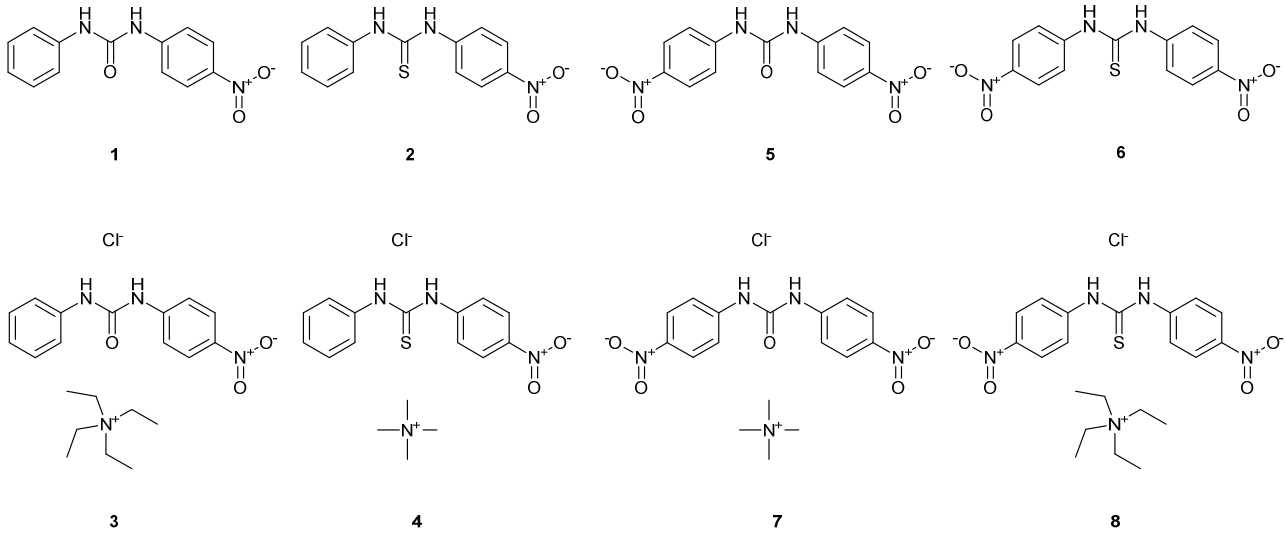

Figure 1. Anion-receptor molecules (**1**, **2**, **5** and **6**) and the chloride complexes of these receptors (**3, 4, 7** and **8**).

Experimental

Synthesis

The synthesis of compound **5** has been previously reported[7].

*1-(4-nitrophenyl)-3-phenylurea (**1**):*

The compound was synthesized according to the adapted procedure of Miyahara.[11] 4- nitrophenylisocyanate (0.5 g, 3.05 x 10^{-3} moles, 1 eq) was dissolved in toluene (70 mL). To this was added aniline (0.25 mL, 3.05 x10^{-3} moles, 1 eq). A white precipitate formed. This was stirred overnight at room temperature under a nitrogen atmosphere. The solid was filtered and dried under vacuum (white solid, 0.73 g, 2.84 x10^{-3} moles, 94 %). MP: 212-214°C (consistent with literature value of 210-211°C)[12]. ^{1}H NMR (300 MHz, d_6-DMSO): 7.02 ppm (t, 0.75 Hz, 1H), 7.31ppm (t, 7.91 Hz, 2H), 7.47 ppm (d, 7.54 Hz, 2H), 7.69 (d, 9.42 Hz, 2H), 8.19 ppm (d, 9.04 Hz, 2H), 8.90 ppm (s, 1H), 9.42 (s, 1H) (consistent with literature reference)[12].

*1-(4-nitrophenyl)-3-phenylthiourea (**2**):*

The compound was synthesized according to the adapted procedure of Perveen *et al*.[13] Aniline (0.23 mL, 2.78 x 10^{-3} moles, 1 eq) was dissolved in dichloromethane (35 mL). 4-nitrophenylisothiocyanate (0.5 g, 2.78 x 10^{-3} moles) dissolved in dichloromethane (35 mL) was added. The yellow solution was left to stir overnight at room temperature under a nitrogen atmosphere. The solvent was removed *in vacuo*, and a yellow solid formed. This was recrystallised from ethanol. The solid was filtered and washed and yielded a yellow solid (0.36 g, 1.32 x10^{-3} moles, 48 %). MP: 150-152°C (consistent with literature value of 145-146 °C).[14] ^{1}H NMR (300 MHz, d_6-DMSO): 7.17 ppm (t, 7.54 Hz, 1H), 7.37 ppm (t, 7.54 Hz, 2H), 7.49 ppm (d, 7.54 Hz, 2H), 7.84 ppm (d, 9.2 Hz, 2H), 8.20 ppm (d, 9.04 Hz, 2H), 10.26 ppm (br. s., 1H), 10.36 ppm (br. s., 1H) (consistent with literature reference)[14].

*1,3-bis(4-nitrophenyl)thiourea (**6**):*

The compound was synthesized according to the procedure of Perveen *et al.*,[13]. 4-nitrophenylisothiocyanate (0.18 g, 1.00 x10^{-3} moles, 1.0 eq) was dissolved in pyridine (5 mL) and 4-nitroaniline (0.20 g, 1.45 x10^{-3} moles, 1.5 eq) in pyridine (5 mL) was added. The clear orange solution was stirred overnight under a nitrogen environment. The solvent was removed *in vacuo* and the resulting solid dissolved in ethyl acetate and washed with 1M HCl and the organic and aqueous layers separated. The organic layer was washed with saturated sodium bicarbonate followed by brine. The organic layer was then dried over $MgSO_4$. After filtration, the solvent was removed *in vacuo* and the solid purified by recrystallisation from ethyl acetate/hexane. This resulted in a yellow solid (0.096g, 3.02 x10^{-4} moles, 30%). MP: 193-196°C (consistent with literature value of 195-196°C).[15] ^{1}H NMR (300 MHz, d_6-DMSO, δ = ppm): 7.85 (d, J=8.8 Hz, 4H, CH), 8.24 (d, J=8.8 Hz, 4H, CH), 10.77 (br. s, 2H, NH) (consistent with literature values)[16].

Crystallisations

Compound **1** was suspended in methanol. TMA chloride was added in methanol and led to full dissolution of the solution. Crystals of receptor **1** then grew upon slow evaporation of the solution. Compound **2** was dissolved in methanol. Vapour diffusion of diethyl ether into the solution resulted in crystals. Crystals of **3** were grown by the vapour diffusion of diethyl ether in an acetonitrile solution of TEA chloride and 1-(4-nitrophenyl)-3-phenylurea. Crystals of **4** were grown by vapour diffusion of diethyl ether into a mixed methanol and ethanol solution of TMA chloride and 1-(4-nitrophenyl)-3-phenylthiourea. **5** was dissolved in acetonitrile and methanol. Crystals formed upon slow evaporation of the solvent mixture. Crystals of **6** were grown by dissolving **6** in acetonitrile and acetone with gently heating. The undissolved solid was filtered and the filtrate was left for the solvent to slowly evaporate. Crystals of **7** were grown as described previously[7] by vapour diffusion of diethyl ether into a solution of TMA chloride and 1,3-bis(4-nitrophenyl)urea. Crystals of **8** were grown by slow evaporation of an acetonitrile solution of TEA chloride and 1,3-bis(4-nitrophenyl)thiourea.

Discussion of the crystal structures of the receptors **1**, **2**, **5** and **6** is given in Section 5 of the ESI†.

View Article Online
DOI: 10.1039/C5CE00213C

X-ray data collection

X-ray data for **1**, **2**, **4**, **5**, **6** and **8** were collected using methods described previously on a Rigaku AFC 12 diffractometer, mounted on a Rigaku FR-E+ Super Bright Very High Flux rotating anode, equipped with a Saturn 724+ CCD detector.[17] For **4** and **8** high quality high resolution data were collected according to a strategy using two detector settings of 2θ which gave overall redundancy of 5.8 and data completeness to $sin\theta/\lambda$ = 1.1 Å^{-1} of 97.0% for **4**; overall redundancy of 5.7 and data completeness to $sin\theta/\lambda$ of 1.05 Å^{-1} of 97.7% for **8**. These resolution of data were chosen as the cut off according to the rules of Herbst- Irmer.[18] X-ray data for **3** was collected on the I19 beamline at the Diamond Light Source[19] using a Crystal Logic 4-kappa diffractometer equipped with a Rigaku Saturn 724+ CCD detector. Following integration in CrystalClear[20], all datasets were scaled and data merged using SORTAV[21].

Despite using synchrotron radiation, it was not possible to obtain high resolution diffraction data for **3** of sufficient quality to allow a full multipole model refinement. This dataset was subsequently subjected to an Invariom refinement using the block matrix technique outlined by Dittrich and co-workers (see below)[10]. Information for the data collection of **7** is given in the literature.[8]

The crystal structures were initially solved by direct methods and refined using the independent atom model IAM (refinement based on F^2) using SHELXL[22] in the WinGX suite[23]. Crystallographic details of **3**, **4**, and **8** can be found in Table 1 as this paper deals primarily with the high resolution crystal structures. The full crystallographic details for the remaining standard resolution crystal structures (**1**, **2**, **5** and **6**) are found Table S5 of the ESI†.

Table 1. Crystallographic details of structures anion-receptor complexes studied at high resolution (for **7** reported elsewhere[8])

Structure	**3** **Invariom refinement**	**4** **High resolution**	**8** **High resolution**
	Independent Atom Model refinement		
Molecular formula	$C_{21}H_{31}ClN_4O_3$	$C_{30}H_{34}ClN_7O_4S_2$	$C_{34}H_{40}ClN_9O_8S_2$
Weight (g mol^{-1})	422.95	656.21	802.32
System	Monoclinic	Triclinic	Triclinic
Space group	$P\,2_1/n$	$P\,\bar{1}$	$P\,\bar{1}$
a (Å)	8.410 (6)	9.159 (1)	8.968 (2)
b (Å)	24.362 (18)	10.244 (2)	15.649 (4)
c (Å)	11.143 (8)	17.871 (3)	15.899 (4)
α (°)	90	87.983 (6)	113.061 (1)
β (°)	106.286 (7)	79.043 (5)	103.685 (3)
γ (°)	90	72.220 (2)	101.701 (2)
V (Å)	2191 (3)	1566.9 (4)	1882.6 (8)
Z	4	2	2
D (g cm^{-3})	1.282	1.391	1.415
Temp (K)	100 (2)	100 (2)	100 (2)
λ	0.68890	0.71073	0.71073
μ (mm^{-1})	0.185	0.303	0.276
F(000)	904	688	840
Crystal	Colourless Tablet	Yellow Plate	Yellow Prism
Crystal size (mm^3)	0.07 x 0.04 x 0.02	0.80 x 0.20 x 0.10	0.31 x 0.27 x 0.12
Data completeness	99.9	96.4	97.7
R_{merge}	0.0832	0.0407	0.0476
Index ranges	$-13 \le h \le 13$ $0 \le k \le 39$ $0 \le l \le 17$	$-22 \le h \le 22$ $-25 \le k \le 25$ $0 \le l \le 44$	$-21 \le h \le 20$ $-38 \le k \le 34$ $-0 \le l \le 38$
T_{min}/T_{max}	0.9859/ 0.9959	0.7935/ 0.9703	0.9194/ 0.9677
Final R indices [$F^2 > 2\sigma(F^2)$]	R1 = 0.0572 *w*R2 = 0.1430	R1 = 0.0531 *w*R2 = 0.1456	R1 = 0.0561 *w*R2 = 0.1369
R indices (all data)	R1 = 0.0636 *w*R2 = 0.1528	R1 = 0.0585 *w*R2 = 0.1506	R1 = 0.0603 *w*R2 = 0.1406
Data/ restraints/ parameters	9511/ 0/ 262	49621/ 0/ 397	55445/ 0/ 487
Δρ(r) (*e* Å^{-3})	0.704/ -0.366	0.941/ -1.009	1.428/ -1.286
	Aspherical Atom Model refinement		
R(F)	0.0450	0.0348	0.0396
R(F^2)	0.0927	0.0378	0.0544
GoF	1.8307	1.7461	2.5564
$(\sin\theta/\lambda)_{max}$	0.77	1.10	1.05
N_{ref}/N_{var}	46.22	27.89	24.43
Δρ(r) (*e*Å^{-3})	0.435/ -0.300	0.650/ -0.557	0.674/ -0.729

Multipole modelling of thiourea complexes 4 and 8

The IAM for **4** and **8** were transferred to the XD2006 suite[24] for full multipole refinement using the Hansen-Coppens formalism[9]. The core and valence scattering factors for the atoms were derived from the Clementi-Roetti wave functions.[25] The refinement was performed on F for all reflections with I > 3σ(I). Initially, only the scale factor was refined against the whole resolution range of diffraction data. Subsequently the positional and anisotropic displacement parameters of the non-hydrogen atoms were refined against the reflections with $\sin(\theta)/\lambda > 0.7$ Å^{-1}. The positions of the hydrogen atoms and their isotropic displacement parameters were then refined against the reflections with $\sin(\theta)/\lambda < 0.7$ Å^{-1}. The X−H distances were then extended along the bond vector to standard lengths for the appropriate functional group as determined from neutron diffraction studies[26]. The anisotropic displacement parameters for each hydrogen atom in the crystal structure were then determined using the SHADE[27] (Simple Hydrogen Anisotropic Displacement Estimator) server. These were imported into the multipole model and fixed throughout the subsequent refinement steps. Next, multipole populations were introduced, with the level of multipole gradually increased from monopole up to the final level: hexadecapole for heteroatoms while those of the carbon atoms were truncated at the octopole level. For hydrogen atoms a single bond directed dipole population was refined. For non-hydrogen atoms excluding sulfur an expansion (κ) parameter was refined while κ' was fixed as 1.00. Chemically equivalent atoms were constrained to share the same expansion/ contraction

View Article Online
DOI: 10.1039/C5CE00213C

parameters. For hydrogen the kappa values were fixed to values of $\kappa = \kappa' = 1.20$. A local coordinate axis system similar to that previously reported was used.[8] The correct modelling of sulfur has been known for some time to be problematic and has been discussed in detail in the charge density community[9,28,29,30] and therefore optimal radial-function parameters may not be the defaults of the XD2006 programme suite.[9] Following the work of Espinosa *et al.*,[28] and Dominiak and Coppens[29] a series of n(l) values were tested, however n(1, 2, 3, 4) = 4 4 4 4 gave the best model for the electron density at sulfur and so was retained in the refinement. Despite this, the residual density at the sulfur atoms was shown to still be quite significant and anharmonic motion modelling using Gram Charlier coefficients was attempted. However this did not improve, and in some cases increased, the residual density. Introduction of a κ' parameter did significantly lessen the residual density and was incorporated into the model. The residual density was shown to be a related to the resolution of the data, as revealed by truncation at different levels (around 0.3/ -0.3 at 0.8 Å^{-1} and 0.6/ -0.6 at 1.1 Å^{-1} for crystal structure **4**). The κ' value was constrained as unconstrained multipole refinement led to physically unreasonable values. In the final stages of the refinement all parameters were refined together with the exception of the κ and κ' values, which were fixed. This led to full convergence of the multipole model. The X-ray data used in the refinement was truncated to an appropriate $\sin(\theta)/\lambda$ limit as outlined by Herbst-Irmer *et al.*[19] As previously discussed,[8] unconstrained refinement of the nitro groups produced a chemically unreasonable range of $\nabla^2\rho(r_{BCP})$ values and hence *mm2* symmetry constraints for the nitrogen atoms of these groups were imposed and the two oxygen atoms in each nitro group were constrained to be chemically identical. The quality of the final model is indicated by the low R(F) and GoF value. The Gaussian distribution of the residual electron density (see fractal dimension distribution plots[31] in the ESI†) suggests that the residual density is noise and that the electron density has been successfully fitted. The high data: parameter ratios demonstrate that sufficient diffraction data has been collected and that overfitting of the model has been avoided.

Invariom Refinement of crystal structure 3

Due to the rapid fall-off of diffraction intensity at high resolution for **3**, despite the use of synchrotron radiation, an X-ray diffraction data set of the required quality for a conventional aspherical atom refinement could not be completed. However, several authors have reported the use of databases of transferable multipole parameters to assist in modelling the electron density distribution where data cannot be obtained of sufficient quality.[32-34] The approach of Dittrich and co-workers was used in this study.[35] The model derived from the independent atom model was transferred to the XD2006 suite[24]. The pre-processor programme InvariomTool[36] was used to assign the multipole parameters and kappa values for each atom which were incorporated into the model. InvariomTool[36] was used to provide the coordinate axes, along with chemical equivalences and local site symmetries. A block refinement was then conducted: positional and anisotropic thermal displacement parameters for the non-hydrogen atoms were refined against all the reflections and subsequently the positions and isotropic thermal displacement parameters for the hydrogen atoms were refined against the low angle data. The scale factor was then refined. This was followed by the refinement of the multipole parameters, with the site symmetry and chemical equivalence constraints maintained, while the kappa parameters were kept fixed to those values obtained from the Invariom database. The quality of the final refinement is illustrated by the values of the R(F) and GoF given in Table 1.

Quantitative analysis of the static electron density model of **3**, **4**, **7** and **8** was performed with the XDPROP module of the XD2006 software suite.[24]

Theoretical Quantum Mechanics Studies

To test the validity of the Invariom modelling of **3,** DFT computational studies were performed on all four anion receptor-complexes (**3**, **4**, **7** and **8**) using the Guassian98 software package[37]. The B3LYP[38,39] /6-311++G**[40] basis set with diffuse functions was used to correctly model the hydrogen atoms and hydrogen bonding in this system. The resulting electron density distribution was analysed using the AIM2000 suite[41]. Critical point analysis for both the computationally and experimentally derived electron density distribution can be found in the ESI†. The properties of the electron density at the bond critical points from these theoretical studies match fairly well with those of the experimental electron density distribution, except for the C=S/ C=O bonds (see Birkedal *et al.*[42] for explanation) and N—O bonds of the nitro groups. This gives a good degree of confidence in the use of the Invariom values used.

Results and Discussion

Solution state studies

Hydrogen bonding

The strength of the association of receptors **1**, **2**, **5** and **6** for chloride was tested in solution in a 0.5% H_2O d_6-DMSO solvent mixture. To satisfy solubility requirements the chloride was added as the tetrabutylammonium salt. The affinity of the thiourea receptors was lower than for the urea receptors and stronger affinity was observed for the symmetrically substituted receptors (**5** > **1** and **6** > **2**). It suggests the number of electron-withdrawing substituents significantly impact on the anion affinity of this receptor.

For each receptor the data fitted well to a 1:1 model (see fit plots in Section 4 of the ESI†). The K_a shown in Table 2 for receptors **1** and **2** were calculated by following the chemical shift of the urea N−H hydrogen atom attached to the nitro-substituted phenyl ring. However, these values are consistent with those for the urea N−H hydrogen atom attached to the unsubstituted ring.

View Article Online
DOI: 10.1039/C5CE00213C

Table 2. Affinity constants (K_a) of the receptors with TBACl in a 0.5% H_2O d_6-DMSO solvent mixture

Receptor	TBACl
1	58 (9%)
2	32 (4%)
5	118 (2%)
6	50 (1%)

Due to the observation of a 2:1 receptor:anion ratio in the solid-state thiourea complexes, Job plots (see ESI†) were constructed to test the ratio of components in the complexes and how they were interacting in solution. These suggested the presence of a 2:1 receptor: anion complex in the equilibrium mixture of the thiourea receptors. Crystal packing effects may account for the fact that this species is observed in the X-ray diffraction studies. However, no fit could be made to a 2: 1 receptor: anion ratio when modelling the titration data.

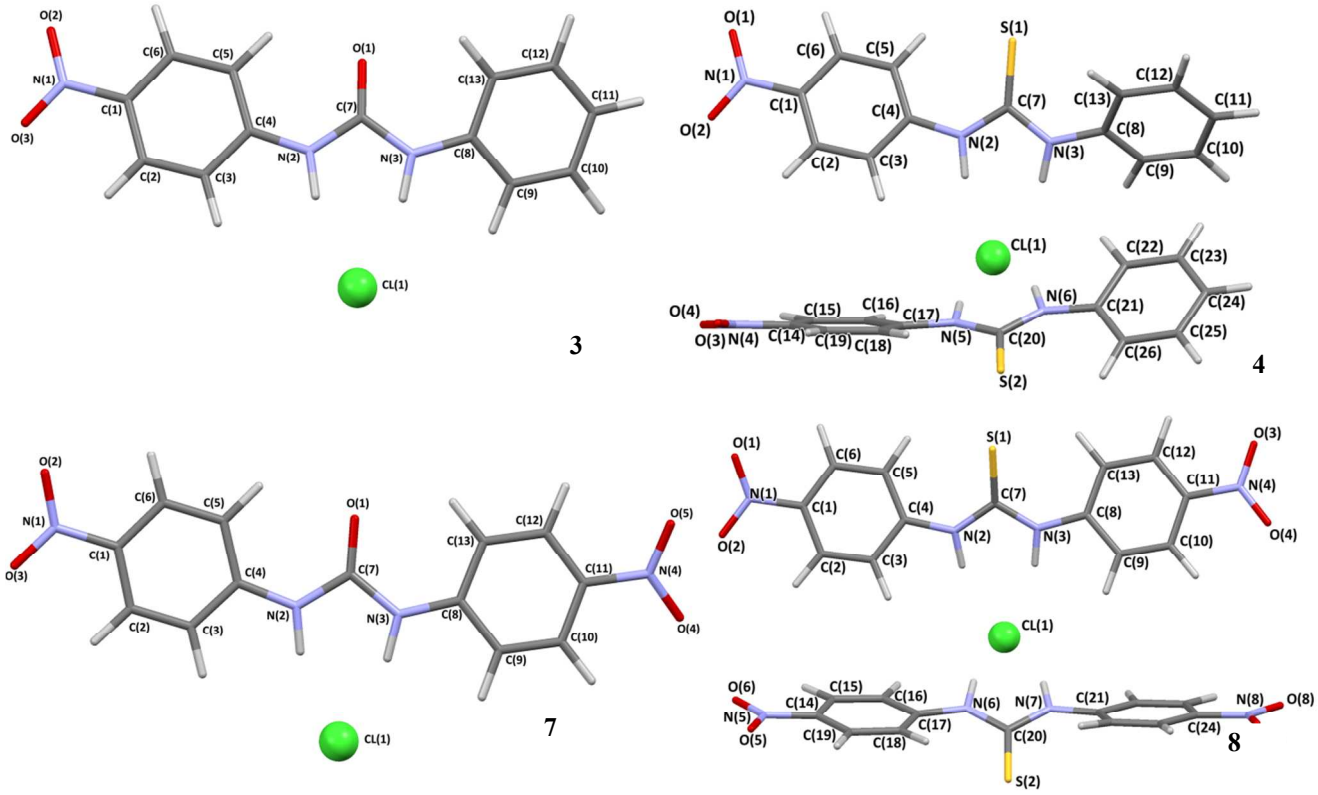

Figure 2. Crystal structures **3**, **4**, **7** and **8** drawn as capped sticks with chloride anion as ball and stick. The cations have been omitted for clarity.

Description of atomic resolution structures

Crystal structures **3** and **7** are both 1:1 anion:receptor complexes, while in **4** and **8** the overall anion: receptor ratio is 1:2 as shown in Figure 2. The packing in **3** arises from $N_2O\cdots$TEA, TEA$\cdots$C=O, Cl$\cdots$TEA and $N_2O\cdots$CH(phenyl) contacts. Similar interactions are observed in **7**, with TMA replacing TEA. The thiourea-based receptors display differences in the crystal structure packing compared to the urea structures. In **4** the chloride anion is complexed by two ligands and therefore not involved in any other interactions. There are S$\cdots NO_2$ and S$\cdots$TMA contacts and T-shaped type π-π interactions between the phenyl rings. In **8** S$\cdots$TEA, TEA$\cdots NO_2$ contacts are accompanied by Cl$\cdots$TEA contacts. It is interesting to note that the sulfur atoms and each receptor molecule in both thiourea complexes (**4** and **8**) are crystallographically independent and distinct. As such it would be expected that the electron density distribution will differ between these receptor molecules.

Hydrogen bonding

The hydrogen bonding in these systems has been carefully analysed (see Table 3). In the receptor structures of the asymmetrically substituted receptors (**1** and **2**, see Figure 3) a chelation of the acceptor part of the (thio)urea by the N−H donor group is observed. However, in the urea structure (**1**) this is a strong α-tape motif, with the D$\cdots$A distance for each hydrogen bond less than the combined van der Waals radii of the donor and acceptor atoms (2.847(4) & 2.883(3) Å). In **2** (the thiourea receptor alone) the D$\cdots$A distance is longer than the combined Van der Waals radii (3.514(2) & 3.461(2) Å) and this accounts for the zig-zag conformation observed.

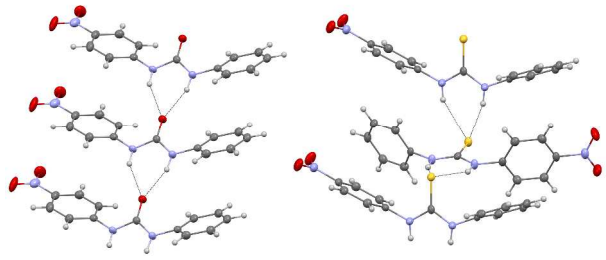

Figure 3. Tape formation in the asymmetric receptor crystal structures **1** (*left*) and **2** (*right*).

It is interesting to note in the crystal structures of the

View Article Online
DOI: 10.1039/C5CE00213C

symmetrical 1,3-bis(4-nitrophenyl)urea and 1,3-bis(4-nitrophenyl)thiourea receptors (**5** and **6**) that this tape motif is replaced by $N_2O\cdots NH$(urea) interactions (this is graphically displayed in the ESI† in figures S28, S29 and S30).[43] This is attributed to the effect of the symmetrical substitution of the receptor.

In all four structures the chloride anion is chelated by hydrogen bonds from the (thio)urea N—H hydrogen bond donor groups. As described previously[7] two hydrogen bonds are present in the urea structures (**3** and **7**) and four hydrogen bonds in the thiourea complexes (**4** and **8**). The asymmetric nature of the receptor may have an effect on the hydrogen bond donor motif, with the distances of the hydrogen bonds involving the N—Hs attached to the nitro substituted phenyl ring shorter than those involving the N—H bonds attached to the unsubstituted phenyl ring in both **3** and **4**. However, there is also variation in the hydrogen bond distances in the symmetrically substituted receptors (**7** and **8**) and therefore geometric arguments are not enough to definitively state the full effect of asymmetric substitution on hydrogen bond strength.

Table 3. Hydrogen bonding distances for **3, 4**, **7** and **8**

Crystal Structure	H···A (Å)	D···A (Å)	∠ DHA (°)
3	2.37	3.223 (2)	161.8
	2.41	3.246 (2)	157.9
4	2.31	3.178 (1)	169.6
	2.43	3.273 (1)	160.7
	2.33	3.168 (1)	158.9
	2.39	3.246 (1)	165.1
7	2.37	3.206 (1)	158.1
	2.33	3.160 (1)	158.0
8	2.50	3.344 (1)	162.2
	2.42	3.276 (2)	165.5
	2.28	3.149 (1)	167.7
	2.38	3.223 (1)	159.5

Hirshfeld surface analysis

The nature of the packing and the relative contributions of the intermolecular interactions in each crystal were further investigated by Hirshfeld surface analysis.[44, 45] The Hirshfeld surfaces and fingerprint plots of the asymmetric crystal structures (**3** and **4**) are shown in Figure 4 while Figure 5 demonstrates the contribution of each interaction type to the Hirshfeld surface. These show that, in each case, upon anion binding the packing efficiency in the crystal structure decreases, as the fingerprint plots of **3** and **4** (urea and thiourea chloride complexes) are more diffuse at higher distances than in **1** and **2**. The shape of the fingerprints plots for **2** and **4** (thiourea receptor molecule and thiourea complex) are relatively similar, while for the urea receptor the change in the fingerprint plot upon anion binding is fairly dramatic with the loss of the O···H tips, which correspond to the nitro···NH(urea) contacts. From the plots of the relative contributions of each interaction to the Hirshfeld surface, it is also observed that the O···H interactions' contribution markedly decreases upon anion binding in both the urea (29.5% in **1** compared to 15.8% in **3**) and thiourea (18.8% in **3** in comparison to 11.8% in **4**) structures. This is accompanied by an increase in the contribution of the H···H contacts (28.8% increases to 51.9% in **3** and 30% in **2** to 36.9% in **4**). In the complexes the Hirshfeld surfaces are mainly comprised of H···H and C···H interactions, with smaller but valuable contributions from H···Cl and O···H contacts. This behaviour is mirrored in the crystal structures of the receptors (**5** and **6**) and anion-receptor complexes (**7** and **8**) of the symmetrical receptors (see ESI† figures S31, S32, S33 and S34 for the plots of these receptors).

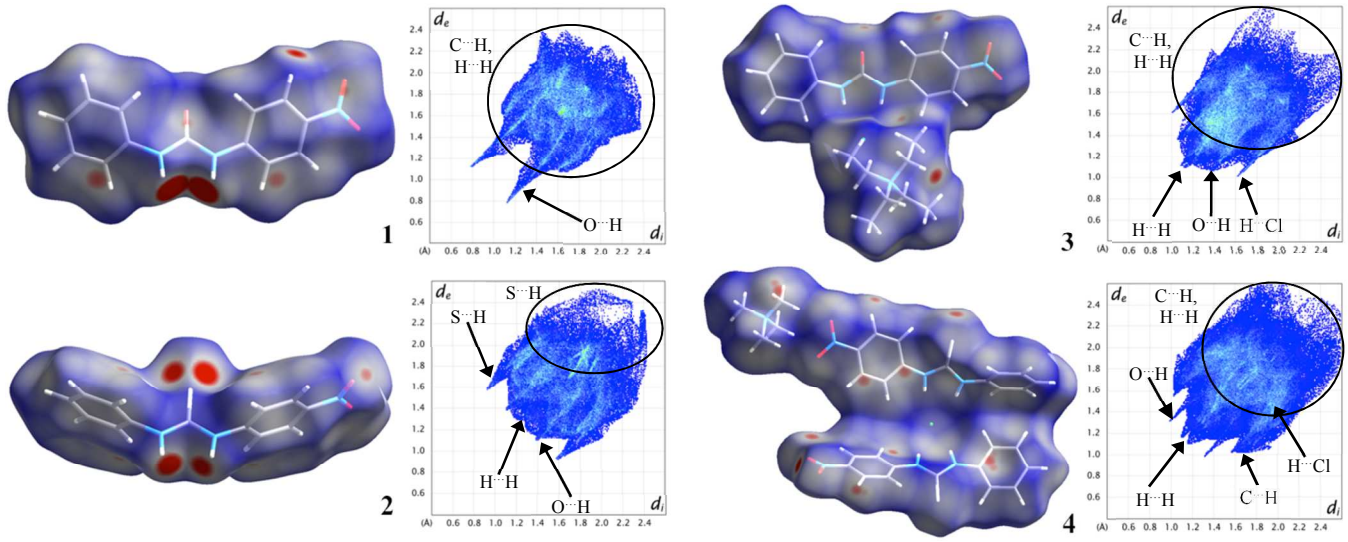

Figure 4. Hirshfeld surface maps and fingerprint plots of receptors (**1** and **2**) and anion-receptor complexes (**3** and **4**)

View Article Online
DOI: 10.1039/C5CE00213C

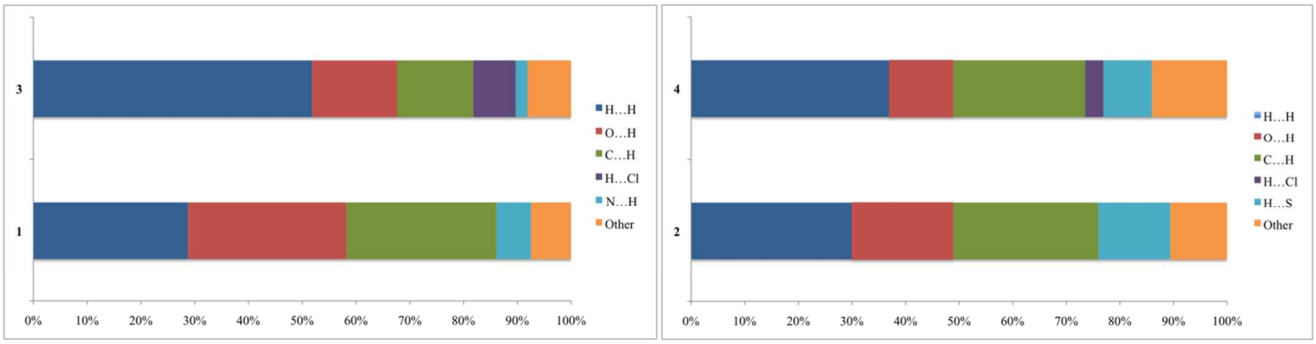

Figure 5. Contribution of non-covalent interactions to the Hirshfeld surface in the urea-based structures (**1** and **3**) and thiourea-based structures (**2** and **4**)

Electron density distribution

In order to further investigate the effects of the altered substitution pattern and the urea *versus* thiourea comparison in a quantitative manner the experimental electron density distributions in all four crystal structures (**3**, **4**, **7** and **8**) were contrasted. For each structure full topological analysis of the bonding was performed and Bader charges for all the atoms in the structures calculated. (See ESI† Section 7 for tables of the atomic charges and the properties of the electron density at the BCPs for the covalent bonds in each structure.)

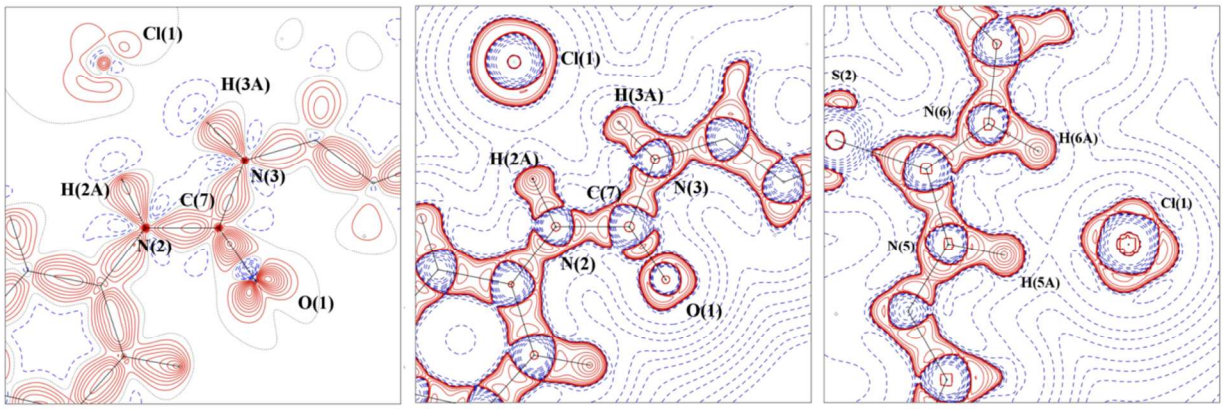

Figure 6. Static deformation density plot of **3** in the plane of the urea molecule (*left*), $-\nabla^2\rho(r)$ map of **3** in the plane of the urea molecule (*middle*), and **4** (right). Positive density shown in red, negative density in blue. Zero contours are dashed. Contours are at 0.1 *e* Å^{-3} for static deformation density plot and in a logarithmic scale, *e* Å^{-5} in the $-\nabla^2\rho(r)$ maps.

General structural features of anion-receptor complexes

Common features of each anion-receptor complex were expected to be similar for **3**, **4**, **7** and **8** and fit with the values described in previous work on bis-substituted receptors (which includes **8**)[8]. Chemical intuition would lead one to predict differences between the urea (**3** and **7**) and thiourea (**4** and **8**) receptors and symmetric (**7** and **8**) and asymmetric (**3** and **4**) receptors (vide infra). As expected, the tetraalkylammonium cation in both asymmetric structures is positively charged (in **3** TEA has 0.268 *e* charge and in **4** TMA is 0.376 *e*) and positively charged in **7** (0.367 *e*) and carries a slight negative charge (-0.050 *e*) in **8**. The chloride anion is negatively charged in all four structures (-0.455 *e* in **3**, -0.066 *e* in **4**, -0.296 *e* in **7** and -0.163 *e* in **8**). The electronic properties of the bonds in key structural areas of the anion receptor complexes, the phenyl rings and (thio)urea moieties were assessed. The average values of the electron density ($\rho(r_{BCP})$) and the Laplacian of the electron density ($\nabla^2\rho(r_{BCP})$) at the BCPs (bond critical points) of the bond paths for these covalent bonds are shown in Table 4 below. They are both comparable across the two types of receptor and consistent with values obtained in previous related studies.[8]

As in the earlier study[8], the carbon atoms of the phenyl rings to which the (thio)urea is bonded carry a highly positive charge in all four structures. Where the nitro group is attached to the phenyl ring the carbon atom has a strong positive charge in all cases (except one position in **8**), while the analogous *para* position on the unsubstituted phenyl ring has a much lower (as in structure **3**) or negative (the case in structure **4**) charge. As would be expected for the nitro groups, the oxygen atoms are highly negative and the nitrogen atoms positively charged.

Hydrogen bonding

The presence of hydrogen bonding between the (thio)urea groups and the chloride anion in each crystal structure was determined by the presence of BCPs associated with each hydrogen bonding interaction and these were analysed by QTAIM[46] (see ESI† Section 8). The energetic properties of the hydrogen bonds; the local kinetic energy density ($G(r_{BCP})$), the local potential energy density ($V(r_{BCP})$), the total energy density ($H(r_{BCP})$) and the hydrogen bond energy (E_{HB}) have been derived (see Table 5)[47] and demonstrate that the hydrogen bonding in this set of structures is weak, closed shell and

View Article Online
DOI: 10.1039/C5CE00213C

electrostatic in nature ($|V(r_{BCP})|/G(r_{BCP}) < 1$, $\nabla^2\rho(r_{BCP})$ and $H(r_{BCP}) > 1$).[48]

An interesting observation is that in both **3** and **4** the strength of the hydrogen bonds are dependent on the substitution of the phenyl ring to which the N—H hydrogen bond donor group is attached. Where there is a nitro group present, the value of the electron density and Laplacian of the electron density at the bond critical point are increased when compared to those values for the hydrogen bonds of the (thio)urea groups attached to an unsubstituted phenyl ring. The bond path length (Rij) is also elongated for the hydrogen bond donor group on the non-substituted side of the receptor. This is a direct observation of the hydrogen bond donor strengthening being caused by electron-withdrawing substituents. The fact that the chloride anion is bound by two thiourea receptor molecules in **4** produces a total hydrogen bonding strength in **4** greater than that in **3**.

The values of the electron density and Laplacian of the electron density at the BCPs do not vary so greatly in the symmetrically substituted receptor complexes (**7** and **8**). However, in **8** (the thiourea complex) there do appear to be differences in the strength of the hydrogen bonding in each of the thiourea molecules present in the crystal structure. This is most likely caused by the distinct crystallographic environment of the thiourea group in the structure.

Table 4. Properties of the electron density at the BCPs for common functional groups in **3**, **4**, **7** and **8**.

Bond type	$\rho(r_{BCP})$ (e Å^{-3})	$\nabla^2\rho(r_{BCP})$ (e Å^{-5})	Rij (Å) Bond Path length
Urea Complex **3**			
C−O urea	3.0	-32.6	1.2216
Phenyl rings nitro substituted C−C bonds	2.2	-18.4	1.3957
Phenyl rings non-nitro substituted C−C bonds	2.1	-16.9	1.3985
Phenyl rings nitro substituted C−H bonds	1.8	-17.6	1.0831
Phenyl rings non-nitro substituted C−H bonds	1.8	-16.4	1.0830
Thiourea Complex **4**			
C−S thiourea	1.4	-3.4	1.6797
Phenyl rings nitro substituted C−C bonds	2.1	-16.1	1.3952
Phenyl rings non-nitro substituted C−C bonds	2.2	-17.0	1.3963
Phenyl rings nitro substituted C−H bonds	1.8	-16.4	1.0834
Phenyl rings non-nitro substituted C−H bonds	1.8	-15.1	1.0835
Urea Complex **7**			
C−O urea	3.1	-39.1	1.2237
Phenyl rings nitro substituted C−C bonds	2.1	-17.7	1.3982
Phenyl rings nitro substituted C−H bonds	1.9	-17.6	1.0831
Thiourea Complex **8**			
C−S thiourea	1.5	-3.2	1.6776
Phenyl rings nitro substituted C−C bonds	2.1	-16.8	1.3943
Phenyl rings nitro substituted C−H bonds	1.9	-17.9	1.0835

Table 5. Topological parameters of the NH···Cl hydrogen bonding interactions in **3**, **4**, **7** and **8**

D−H···A	H···A	$\rho(r_{BCP})$ (e Å^{-3})	$\nabla^2\rho(r_{BCP})$ (e Å^{-5})	R_{ij} H···A (Å)	A−BCP distance (Å)	H−BCP distance (Å)	D−BCP distance (Å)	$G(r_{BCP})$ (a.u)	$V(r_{BCP})$ (a.u)	$\lvert V(r_{BCP})\rvert/G(r_{BCP})$	E_{HB} (kJ mol^{-1})	$H(r_{BCP})$ (kJ mol^{-1})
3. ***Unsymmetrical*** *urea receptor with chloride*												
N(2)−H(2A)···CL(1)	H(2A)···CL(1)	0.09(2)	1.974(9)	2.2804	1.5291	0.7514	1.6934	0.016	-0.011	0.6979	-14.41	12.47
N(3)−H(3A)···CL(1)	H(3A)···CL(1)	0.07(2)	1.487(3)	2.4149	1.5929	0.8220	1.6902	0.012	-0.007	0.6628	-10.04	10.21
4. ***Unsymmetrical*** *thiourea receptor with chloride*												
N(2)−H(2A)···CL(1)	H(2A)···CL(1)	0.12(2)	2.107(7)	2.1947	1.4331	0.7616	1.7473	0.018	-0.014	0.779	-18.32	10.37
N(3)−H(3A)···CL(1)	H(3A)···CL(1)	0.09(1)	1.425(2)	2.3555	1.4983	0.8572	1.7759	0.012	-0.009	0.753	-11.71	7.70
N(5)−H(5A)···CL(1)	H(5A)···CL(1)	0.16(2)	2.042(5)	2.1941	1.3953	0.7988	1.7763	0.020	-0.018	0.914	-23.42	4.40
N(6)−H(6A)···CL(1)	H(6A)···CL(1)	0.10(2)	1.718(4)	2.2849	1.4812	0.8037	1.7701	0.015	-0.011	0.774	-14.76	8.63
7. ***Symmetrical*** *urea receptor with chloride*												
N(2)−H(2A)···CL(1)	H(2A)···CL(1)	0.120(1)	1.949(4)	2.2423	1.4656	0.7767	1.744	0.017	-0.014	0.808	-17.98	8.56
N(3)−H(3A)···CL(1)	H(3A)···CL(1)	0.125(2)	2.319(7)	2.1854	1.4562	0.7292	1.705	0.020	-0.016	0.783	-20.30	11.277
8. ***Symmetrical*** *thiourea receptor with chloride*												
N(2)−H(2A)···CL(1)	H(2A)···CL(1)	0.06(3)	1.585(5)	2.4302	1.6135	0.8167	1.7382	0.012	-0.007	0.623	-9.76	11.83
N(3)−H(3A)···CL(1)	H(3A)···CL(1)	0.06(2)	1.589(5)	2.4048	1.5947	0.8101	1.7011	0.012	-0.008	0.629	-9.93	11.71
N(6)−H(6A)···CL(1)	H(6A)···CL(1)	0.09(4)	2.36(2)	2.2070	1.5057	0.7012	1.6475	0.019	-0.013	0.684	-16.69	15.45
N(7)−H(7A)···CL(1)	H(7A)···CL(1)	0.10(3)	2.25(1)	2.2741	1.5122	0.7619	1.7104	0.018	-0.013	0.725	-17.41	13.24

Comparison of urea and thiourea electron density distribution

A major difference in the urea and thiourea receptors is the

View Article Online
DOI: 10.1039/C5CE00213C

properties of the bond critical points of the C=O/C=S bonds. In the urea structures **3** and **7** (electron density and Laplacian of the electron density are ~3.1 *e* Å^{-3} and -36 *e* Å^{-5}) there is agreement but these are different when compared to thioureas **4** and **8**, where the electron density and Laplacian of the electron density at the C−S BCP is substantially different (1.4 *e* Å^{-3} and -3.3 *e* Å^{-5}). This phenomenon is therefore a property of the difference between urea and thiourea, rather than symmetrical nitro substitution to unsymmetrical nitro substitution, arising from the urea C=O bond being more polar in nature than the C=S bond. This reflects the stronger difference in electronegativity between carbon and oxygen as opposed to carbon and sulfur.[49]

The differences in the electron density distribution across the entire molecular ensemble between the urea (**3**, **7**) and thiourea (**4**, **8**) based structures was probed by studying the atomic charges (calculated using QTAIM theory and found tabulated in Section 8 of the ESI†). Additionally the electrostatic potential distributions in the crystal structures, visualised using the MolIso program[50] and shown for **3** in Figure 7 and for **4** in Figure 8, were investigated. The electrostatic potential distributions in **7** and **8** are also included in Section 9 of the ESI† and follow the trends outlined below.

When comparing the two types of receptor (urea *vs.* thiourea), there is a large variation in the electrostatic potential distributions. The electrostatic potential distribution of both the TEA/TMA groups and chloride anions in both **3** and **4** are similar (as in **7** and **8**). The electrostatic potential distribution of the nitro groups varies significantly between **3** (less negative electrostatic potential) and **4** (higher negative electrostatic potential). This matches the trends in the atomic charges of the nitrogen (higher positive charge in **3**) and oxygen atoms (higher negative charge in **4**) in these groups. The most striking difference is the electrostatic potential distributions around the urea and thiourea. In **3** the oxygen has a slightly negative electrostatic potential (matching the charge of this atom (-0.723 *e*)) while the sulfur atoms in **4** have a positive electrostatic potential - again this matches their charges of 0.155 *e* (S1) and 0.651 *e* (S2). This is also detected in the electrostatic potential distributions of **7** and **8**, with the sulfur atoms of **8** carrying charges of 1.166 *e* and -0.099 *e* and the oxygen atom of the urea in **7** a charge of -1.047 *e*. Positive sulfur atoms have previously been observed in the study of a thiadiazole crystal structure, where the authors postulate the positive charge is compensated by negatively charged nitrogen atoms. This is also the case in the thiourea molecules presented herein.[51]

Differences in the electrostatic potential between the two receptor molecules in structure **4** are clearly visible. This is most marked between the two sulfur atoms, which have considerably variable charges (vide supra) and electrostatic potential distributions. This may be linked to the different close contact environments in which the different sulfur atoms are involved (see Table 6). In **4** S(1) participates in interactions with the nitro groups of another thiourea group while S(2) has interactions with the hydrogen atoms of a TMA group. Again, this is also the case in the symmetrical thiourea **8**.

In both **3** and **4** bond paths between the oxygen or sulfur atoms of the (thio)urea moiety and hydrogen atoms in the *ortho* position of the ring indicate that there is an interaction resulting in the formation of a pseudo six-membered ring. These interactions are slightly weaker in **4** than **3**, possibly due to the thiourea receptor molecules in **4** being twisted further out of the plane of the phenyl rings than the urea group in **3**. This is evidenced by a longer bond path length for contacts involving the thioureas (see Table 6). These are present in the crystal structures of both the symmetrically substituted receptor complexes (**7** and **8**), however in the thiourea (**8**) they are only observed in one of the two independent receptor molecules in the crystal structure.

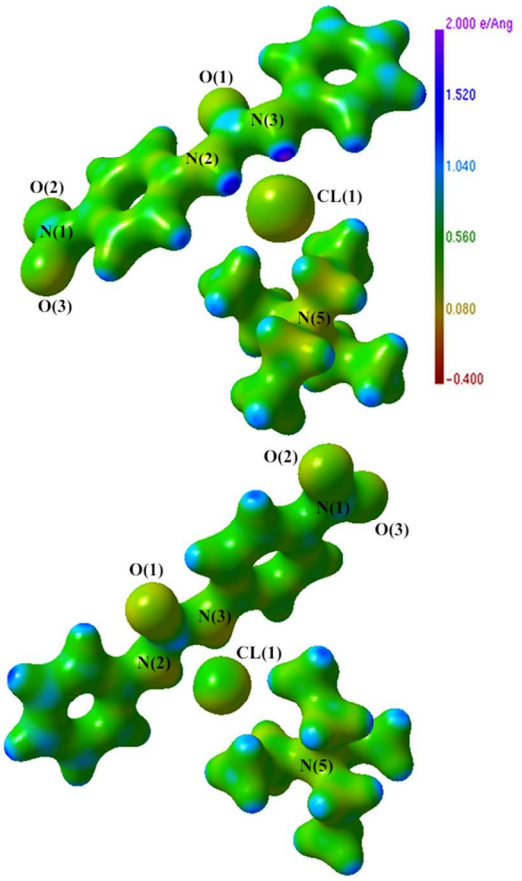

Figure 7. Two views of the electrostatic potential distribution plot[50] (units of *e* Å^{-1}) of crystal structure **3**

View Article Online
DOI: 10.1039/C5CE00213C

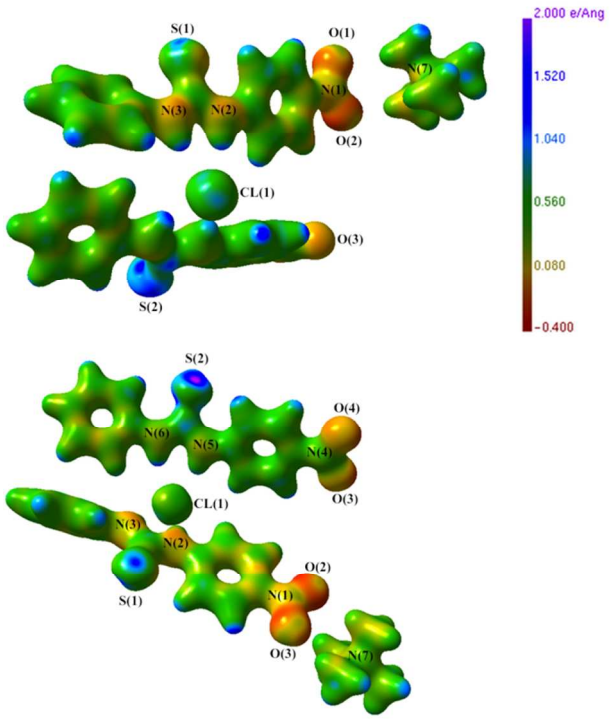

Figure 8. Two views of the electrostatic potential distribution plot[50] (units of e Å^{-1}) of crystal structure **4**

Table 6. Weaker non-covalent interactions in **3**, **4** and **8**

Critical point	$\rho(r_{BCP})$ (e Å^{-3})	$\nabla^2\rho(r_{BCP})$ (e Å^{-5})	R_{ij} (Å)	d_1 A–BCP (Å)	d_2 BCP–B (Å)	ε
Thiourea intermolecular interactions						
4. S(1)···N(4) †	0.049(1)	0.714(2)	3.4984	1.6849	1.8135	0.62
4. S(1)···O(3) †	0.049(1)	0.714(2)	3.1779	1.6849	1.4930	0.62
4. ‡ S(2)···H(72A)	0.020(7)	0.407(3)	2.9296	1.8328	1.0968	0.09
4. ‡ S(2)···H(73A)	0.018(7)	0.341(3)	2.9148	1.7884	1.1264	0.03
8. S(1)···N(7) §	0.035(2)	0.495(3)	3.2624	1.6820	1.5804	0.25
8. δ S(2)···H(96B)	0.05(2)	0.654(5)	2.8488	1.7969	1.0519	0.04
8.ξ S(2)···H(93B)	0.03(2)	0.537(4)	2.8110	1.8312	0.9798	0.09
Intramolecular interactions						
3. O(1)···H(5)	0.115(2)	1.928(5)	2.1722	1.2861	0.8861	0.53
3.O(1)···H(13)	0.101(2)	1.473(4)	2.3485	1.3276	1.0208	0.33
4. S(1)···H(5)	0.094(3)	1.221(3)	2.6491	1.6010	1.0480	0.25
4. S(1)···H(13)	0.076(2)	0.972(2)	2.7812	1.6262	1.1549	0.60
4. S(2)···H(18)	0.084(3)	1.182(3)	2.6042	1.5732	1.0310	0.09
4. S(2)···H(26)	0.071(2)	0.947(3)	2.6512	1.5679	1.0833	0.35

§Symmetry used to generate interaction 1-x, 1-y, 1-z, δsymmetry used to generate interaction -1+x, y, z, ξsymmetry used to generate interaction 2-x, 1-y, 2-z, †symmetry used to generate interaction 1-x, -y, -z ‡ symmetry used to generate interaction 1-x, 1-y, -z.

Comparison of unsymmetrical and symmetrical complexes

A further key comparison is that of asymmetrical (**3** and **4**) *versus* symmetrical substitution (**7** and **8**) of the receptor. Comparing the urea portion of the symmetrical receptor **7** with asymmetrical receptor **3**, the difference between the atoms is less extreme, with the oxygen atom carrying a charge of -0.723 *e* compared to a charge of -1.047 *e* on the 1,3-bis(4-nitrophenyl)urea. Additionally, the two carbon atom charges are 1.260 *e* in **3** and 1.506 *e* in 1,3-bis(4-nitrophenyl)urea. This is due to the lower electron-withdrawing effect exerted on the urea of one nitro group (**3**) compared to two nitro groups in **7**. The nitrogen atoms of the urea were -1.260 *e* and -0.991 *e* in **3** and -1.098 *e* and -1.121 *e* in 1,3-bis(4-nitrophenyl)urea **7**.

When considering the properties of the electron density at the bond critical points for the phenyl rings C—C and C—H bonds in the symmetrical and asymmetrical receptors, the values agree within error. This suggests the effect of the loss of one electron-withdrawing group is hard to detect and that it is a less dramatic change than altering the central anion binding group from a urea to a thiourea (excluding the difference in charges on the carbonyl carbon atoms). This is clearly an important consideration for chemists when designing anion-receptor molecules. However, as has been demonstrated above, the partial loss of an electron-withdrawing unit can weaken hydrogen bond donor abilities of N—H bonds at that portion of the receptor structure.

Conclusions

Anion binding effects dramatic differences between these related crystal structures, as illustrated by Hirshfeld surface analysis. Charge density analysis is able to more thoroughly account for these differences by systematically mapping the electron density distribution across the series. The asymmetrical substitution of the receptor molecules is shown to alter the packing and intermolecular contacts in both the receptor structures and the anion-receptor complexes. However, the variation between urea and thiourea substantially changes the packing and anion binding properties (2:1 receptor:anion in the thiourea complex *versus* 1:1 receptor:anion in the urea complex). In addition, the electron density distribution in the crystal structures significantly alters between thiourea and urea receptors with dissimilarity in atomic charges, electrostatic potential distributions and the properties of the electron density at the BCPs of the (thio)urea groups. These considerable differences help to account for the varying abilities and applications of urea and thiourea molecules as anion-receptors. Hydrogen bond strength in the series of four chloride complexes was determined and shown to be weak in nature and dependent on the position of the hydrogen bond donor group on the asymmetrically substituted receptor. This also differs between thiourea receptor molecules involved in 2:1 receptor anion binding interactions.

Divergence in the electron density distribution, atomic charges and electrostatic potential distribution across two examples containing the same receptor molecule in the thiourea 2:1 complex, illustrates how properties of molecules can vary greatly depending on the crystalline environment.

Notes and references

[a] *Chemistry, University of Southampton, Southampton, UK, SO17 1BJ. E-mail: s.j.coles@soton.ac.uk; philip.gale@soton.ac.uk*
[b] *Diamond Light Source, Diamond House, Harwell Science and Innovation Campus, Didcot, Oxfordshire, UK, OX11 0DF.* Current

View Article Online
DOI: 10.1039/C5CE00213C

address: *School of Chemistry, University of Glasgow, Joseph Black Building, Glasgow, G12 8QQ.*

† Electronic Supplementary Information (ESI) available including NMR titration data, QTAIM charges and theoretical and experimental topological analyses of chemical bonding in the crystal structures. Crystal structures deposited with the Cambridge Crystallographic Data Centre with deposition numbers CCDC1042624-1042633. See DOI: 10.1039/b000000x/

‡ Footnotes should appear here. These might include comments relevant to but not central to the matter under discussion, limited experimental and spectral data, and crystallographic data.

1. P. A. Gale, N. Busschaert, C. J. E. Haynes, L. E. Karagiannidis and I. L. Kirby, *Chem. Soc. Rev.*, 2014, **43**, 205.
2. A.-F. Li, J.-H. Wang, F. Wang and Y.-B. Jiang, *Chem. Soc. Rev.*, 2010, **39**, 3729.
3. M. C. Etter, Z. Urbanczyk-Lipkowska, M. Zia-Ebrahimi and T. W. Panunto, *J. Am. Chem. Soc.*, 1990, **112**, 8415.
4. L. S. Reddy, S. K. Chandran, S. George, N. J. Babu and A. Nangia, *Cryst. Growth Des.*, 2007, **7**, 2675.
5. R. Custelcean, *Chem. Commun.*, 2008, 295.
6. R. Custelcean, M. G. Gorbunova and P. V. Bonnesen, *Chem. Eur. J.*, 2005, **11**, 1459.
7. I. L. Kirby, M. B. Pitak, M. Wenzel, C. Wilson, H. A. Sparkes, S. J. Coles and P. A. Gale, *CrystEngComm*, 2013, **15**, 9003.
8. I. L. Kirby, M. Brightwell, M. B. Pitak, C. Wilson, S. J. Coles and P. A. Gale, *PCCP*, 2014, **16**, 10943.
9. N. K. Hansen and P. Coppens, *Acta Crystallogr., Sect. A.*, 1978, **34**, 909.
10. B. Dittrich, T. Koritsánszky and P. Luger, *Angew. Chem. Int. Ed.*, 2004, **43**, 2718.
11. M. Miyahara, *Chem. Pharm. Bull.*, 1986, **34**, 1950.
12. S. Gavade, R. Balaskar, M. Mane, P. N. Pabrekar and D. Mane, *Synth. Commun.*, 2012, **42**, 1704.
13. S. Perveen, S. M. Abdul Hai, R. A. Khan, K. M. Khan, N. Afza and T. B. Sarfaraz, *Synth. Commun.*, 2005, **35**, 1663.
14. Y.-S. Lin, J.-X. Zheng, Y.-K. Tsui and Y.-P. Yen, *Spectrochim. Acta. A.*, **79**, 1552.
15. E. Dyer, T. B. Johnson, *J. Am. Chem. Soc.*, 1932, **54**, 777.
16. R. Kato, S. Nishizawa, T. Hayashita and N. Teramae, *Tetrahedron Letts.*, 2001, **42**, 5053–5056.
17. S. J. Coles and P. A. Coles, *Chem. Sci.*, 2012, **3**, 683.
18. R. Herbst-Irmer, A. L. Spek, T. Schneider, M. Sawaya and P. Muller, *Crystal Structure Refinement: A crystallographer's guide to Shelxl*, 2006., Oxford Uni. Press, Oxford, UK
19. H. Nowell, S. A. Barnett, K. E. Christensen, S. J. Teat and D. R. Allan, *J. Synchrotron. Radiat.*, 2012, **19**, 435.
20. Rigaku, *CrystalClear- SM Expert 3.1 b27,* 2013
21. R. Blessing, *J. Appl. Crystallogr.*, 1997, **30**, 421.
22. G. Sheldrick, *Acta Crystallogr., Sect. A.*, 2008, **64**, 112.
23. L. Farrugia, *J. Appl. Crystallogr.*, 2012, **45**, 849.
24. XD2006 - A Computer Program Package for Multipole Refinement, Topological Analysis of Charges Densities and Evaluation of Intermolecular Energies from Experimental and Theoretical Structure Factors. A. Volkov, P. Macchi, L. J. Farrugia, C. Gatti, P. Mallinson, T. Richter and T. Koritsanszky, 2006.
25. E. Clementi and C. Roetti, *At. Data Nucl. Data Tables*, 1974, **14**, 177.
26. F. H. Allen, O. Keenard, D. G. Watson, L. Brammer, A. G. Orpen and R. Taylor, *International Tables for X-ray Crystallography*, 2006., Vol. C.
27. A. Madsen, *J. Appl. Crystallogr.*, 2006, **39**, 757.
28. E. Espinosa, E. Molins and C. Lecomte, *Phys. Rev. B.*, 1997, **56**, 1820.
29. P. M. Dominiak and P. Coppens, *Acta Crystallogr., Sect. A.*, 2006, **62**, 224.
30. A. Volkov and P. Coppens, *Acta Crystallogr., Sect. A.* ,2001, **57**, 395.
31. K. Meindl and J. Henn, *Acta Crystallogr., Sect. A.*, 2008, **64**, 404.
32. S. Domagała, B. Fournier, D. Liebschner, B. Guillot and C. Jelsch, *Acta Crystallogr., Sect. A.*, 2012 **68**, 337.
33. K. N. Jarzembska and P. M. Dominiak, *Acta Crystallogr., Sect. A.*, **68**, 139.
34. B. Dittrich, C. B. Hubschle, K. Propper, F. Dietrich, T. Stolper and J. J. Holstein, *Acta Crystallogr., Sect. B.*, 2013, **69**, 91.
35. B. Dittrich, C. B. Hubschle, J. J. Holstein and F. P. A. Fabbiani, *J. Appl. Crystallogr.*, 2009, **42**, 1110.
36. C. B. Hubschle, P. Luger and B. Dittrich, *J. Appl. Crystallogr.*, 2007, **40**, 623.
37. G98: M. J. Frisch, G. W. Trucks, H. B. Schlegel, G. E. Scuseria, M. A. Robb, J. R. Cheeseman, J. A. Montgomery, T. Vreven, K. N. Kudin, J. C. Burant, J. M. Millam, S. S. Iyengar, J. Tomasi, V. Barone, B. Mennucci, M. Cossi, G. Scalmani, N. Rega, G. A. Petersson, H. Nakatsuji, M. Hada, M. Ehara, K. Toyota, R. Fukuda, J. Hasegawa, M. Ishida, T. Nakajima, Y. Honda, O. Kitao, H. Nakai, M. Klene, X. Li, J. E. Knox, H. P. Hratchian, J. B. Cross, V. Bakken, C. Adamo, J. Jaramillo, R. Gomperts, R. E. Stratmann, O. Yazyev, A. J. Austin, R. Cammi, C. Pomelli, J. W. Ochterski, P. Y. Ayala, K. Morokuma, G. A. Voth, P. Salvador, J. J. Dannenberg, V. G. Zakrzewski, S. Dapprich, A. D. Daniels, M. C. Strain, O. Farkas, D. K. Malick, A. D. Rabuck, K. Raghavachari, J. B. Foresman, J. V. Ortiz, Q. Cui, A. G. Baboul, S. Clifford, J. Cioslowski, B. B. Stefanov, G. Liu, A. Liashenko, P. Piskorz, I. Komaromi, R. L. Martin, D. J. Fox, T. Keith, M. A. Al-Laham, C. Y. Peng, A. Nanayakkara, M. Challacombe, P. M. W. Gill, B. Johnson, W. Chen, M. W. Wong, C. Gonzalez and J. A. Pople, 1998.
38. C. Lee, W. Yang and R. G. Parr, *Phys. Rev. B.*, 1988, **37**, 785.
39. A. D. Becke, *J. Chem. Phys.*, 1993, **98**, 5648.
40. P. C. Hariharan and J. A. Pople, *Theor. Chim. Acta.*, 1973, **28**, 213.
41. a) F. Biegler-König, J. Schönbohm and D. Bayles, *J. Comput. Chem.*, 2001, **22**, 545; b) F. Biegler-König and J. Schönbohm, *J. Comput. Chem.*, 2002, **23**, 1489
42. H. Birkedal, D. Madsen, R. H. Mathieson, K. Knudsen, H. -P. Weber, P. Pattison, D. Schwarzenbach, *Acta Crystallogr. Sect. A.*, 2004, **60**, 371.
43. S. George, A. Nangia, C.-K. Lam, T. C. W. Mak and J.-F. Nicoud, *Chem. Commun.*, 2004, 1202.
44. M. A. Spackman and D. Jayatilaka, *CrystEngComm*, 2009, **11**, 19.
45. M. A. Spackman and J. J. McKinnon, *CrystEngComm*, 2002, **4**, 378.
46. R. F. W. Bader, *Atoms-in-Molecules: A Quantum Theory*, 1990, Clarendon Press, Oxford, UK.
47. Y. Abramov, *Acta Crystallogr., Sect. A.*, 1997, **53**, 264.

View Article Online
DOI: 10.1039/C5CE00213C

48. I. Rozas, I. Alkorta and J. Elguero, *J. Am. Chem. Soc.*, 2000, **122**, 11154.
49. F. H. Allen, C. M. Bird, R. S. Rowland and P. R. Raithby., *Acta Crystallogr., Sect. B.*, 1997, **53**, 680.
50. C. B. Hubschle and P. Luger, *J. Appl. Crystallogr.*, 2006, **39**, 901.
51. W. Nakanishi, S. Hayashi, M. B. Pitak, M. B. Hursthouse and S. J. Coles, *J. Phys. Chem. A.*, 2011, **115**, 11775.